


The Occurrence of Chunky Graphite in Ductile Cast Iron Solution Strengthened by Silicon

Artur Zaczyński ^a, Maciej Królikowski ^{a*}, Marek Sokolnicki ^a, Adam Nowak ^a,
Edward Guzik ^b, Andriy Burbelko ^b

^aOdlewnie Polskie S.A., 22 Rogowskiego St., 27-200 Starachowice, Poland

^bAGH University of Krakow, Faculty of Foundry Engineering, 23 Reymonta St., 30-059 Krakow, Poland

* e-mail: maciej.krolikowski@odlewniepolskie.pl

© 2025 Authors. This is an open access publication, which can be used, distributed and reproduced in any medium according to the Creative Commons CC-BY 4.0 License requiring that the original work has been properly cited.

Received: 9 November 2024/Accepted: 26 May 2025/Published online: 30 June 2025.

This article is published with open access at AGH University of Science and Technology Journals.

Abstract

Solution strengthened ferritic cast iron is characterised in EN 1563:2018 (and also in ISO 1083:2018) as grades EN-GJS-450-18, EN-GJS-500-14 and EN-GJS-600-10. Machine and plant builders have been using this material in new designs since 2011. The strength and ductile properties, competitive in comparison with the previous classical ductile cast iron grades, make it possible to reduce the weight of castings. Particularly preferred is grade EN-GJS-600-10 with R_m min. 600 MPa and A min. 10%. Strengthening of the ferritic matrix is possible due to the content of approximately 4.2% of silicon in the cast iron. In casting practice, this material is difficult to produce in a stable manner due to the frequent occurrence of degenerate chunky graphite in the casting structure, resulting in a loss of ductile properties of the cast iron. In this article, an analysis has been made, based on literature, of the occurrence of strong negative segregation of silicon in classical ductile cast iron. The authors' own research has confirmed the occurrence of chunky graphite in the cast. Dendritic crystallisation of austenite and strong segregation of silicon favours the formation of chunky graphite. A much stronger proportion of silicon was found in the chunky graphite zone, compared to the adjacent ball graphite zone. The introduction of micro-additives into the liquid melt eliminated the presence of chunky graphite in the casting. The applied modifiers of graphite and metal matrix (hybrid modification) seem to be an effective method to stabilise the technological process of this innovative casting material.

Keywords:

Silicon reinforced ductile iron, chunky graphite, segregation, hybrid modification

1. STATE OF THE ART

Previous studies of the occurrence of chunky graphite in classic types of ductile cast iron have mostly concerned thick-walled castings [1, 2]. A number of studies were carried out for solution-reinforced silicon. The cast iron grade GJS 600-10, with Si content of approx. 4.2% and C content of approx. 2.8%, is particularly susceptible to graphite degeneration [3]. This often occurs in castings under sprues and in walls with a thickness of over 30 mm. The assessment of the material properties is determined on samples taken from castings. Chunky graphite is a barrier to the implementation of this material in industrial practice.

Given the relatively modest cost of silicon, its use as a reinforcing addition may be of interest from an economic perspective. The phenomenon of chunky graphite formation in silicon-reinforced cast iron was considered in light of existing theories, taking into account the impact of increased silicon content on the crystallization process of cast iron. The strong negative segregation of silicon in cast iron was also taken into account.

The most important theories of the formation of chunky graphite are as follows [1]:

- Liu, Li, Wu, and Loper (1983) explain the formation of chunky graphite due to the preferential growth of graphite along the “c” direction [4].
- Zhou, Schmitz, and Engler (1987) explain the formation of chunky graphite by the accumulation of carbon atoms in the liquid phase between the arms of the dendritic primary austenite [5]. As a consequence, supersaturated carbon areas are created, from which chunky graphite is released.
- Gagné and Argos (1989), crystal growth on the basal plane as helical dislocation [6].
- Itofuji and Uchikawa (1990), with the “place theory”, they suspect the growth of graphite in magnesium vapor bubbles in liquid cast iron [7].
- Källborn, Hamberg, Wessen and Björkegren (2005) believe that chunky graphite appears early during the crystallization of eutectics formed before spheroid separation [8].
- The Wedge Theory according to Udroui (2013) is a new approach to explain the formation of chunky graphite in ductile iron [3].

The procedure of forming chunky graphite according to Zhou et al. in ductile iron is schematically presented in four stages in Figure 1 [1]. This dendritic theory also takes into account the segregation of elements occurring at the crystallization front. Below are these stages:

- Initially, precipitates of primary graphite are formed shortly before reaching the eutectic temperature (stage 1, Fig. 1). Simultaneously and independently, small austenite dendrites (γ) are formed. Nodular graphite precipitates are quickly isolated from the liquid phase by the *austenite envelope*, and their further growth (coupled with the thickening of the austenite envelope) occurs as a result of the carbon diffusion through the solid phase layer.
- Shortly after that the nucleation and growth of chunky graphite grains begins at the surface of the austenite dendrites (stage 2, Fig. 1). There is a simultaneous precipitation of graphite and austenite with loose coupling between graphite and austenite. This mechanism of simultaneous crystallization of both eutectic phases is called growth “with loose coupling between graphite and austenite” in [1].
- The growth of eutectic colonies „ γ + chunky graphite” (stage 3, Fig. 1) causes the enrichment of the liquid adjacent to the crystallization front with components

such as Mg, Si, Mn, Mo, Cr, V, B, Ti. At the same time, nucleation of new eutectic seeds of the same type continues. During eutectic crystallization of this type, both phases are constantly in contact with the disappearing liquid phase.

- Eutectics growth ends (stage 4, Fig. 1). Elements that are less soluble or insoluble in austenite segregate in the residual alloy and influence the crystallization process there. For example, the magnesium available in this area will promote the formation of ductile graphite. Moreover, carbides may be precipitated at the grain boundaries.

An unfavourable phenomenon in ductile cast iron is the direct segregation of C and Mn elements and the strong reverse segregation of Si (Fig. 2). The segregation value is described by the Equation (1) and the parameter K_S (Table 1) [9].

$$K_S = \frac{C_{\text{Austenite}}}{C_{\text{LTF}}} \quad (1)$$

where:

- $C_{\text{Austenite}}$ – concentration of the element in the centre of the austenite dendrite,
- C_{LTF} – concentration of the same element in the areas of the liquid phase where crystallization ends at the lowest temperature (LTF).

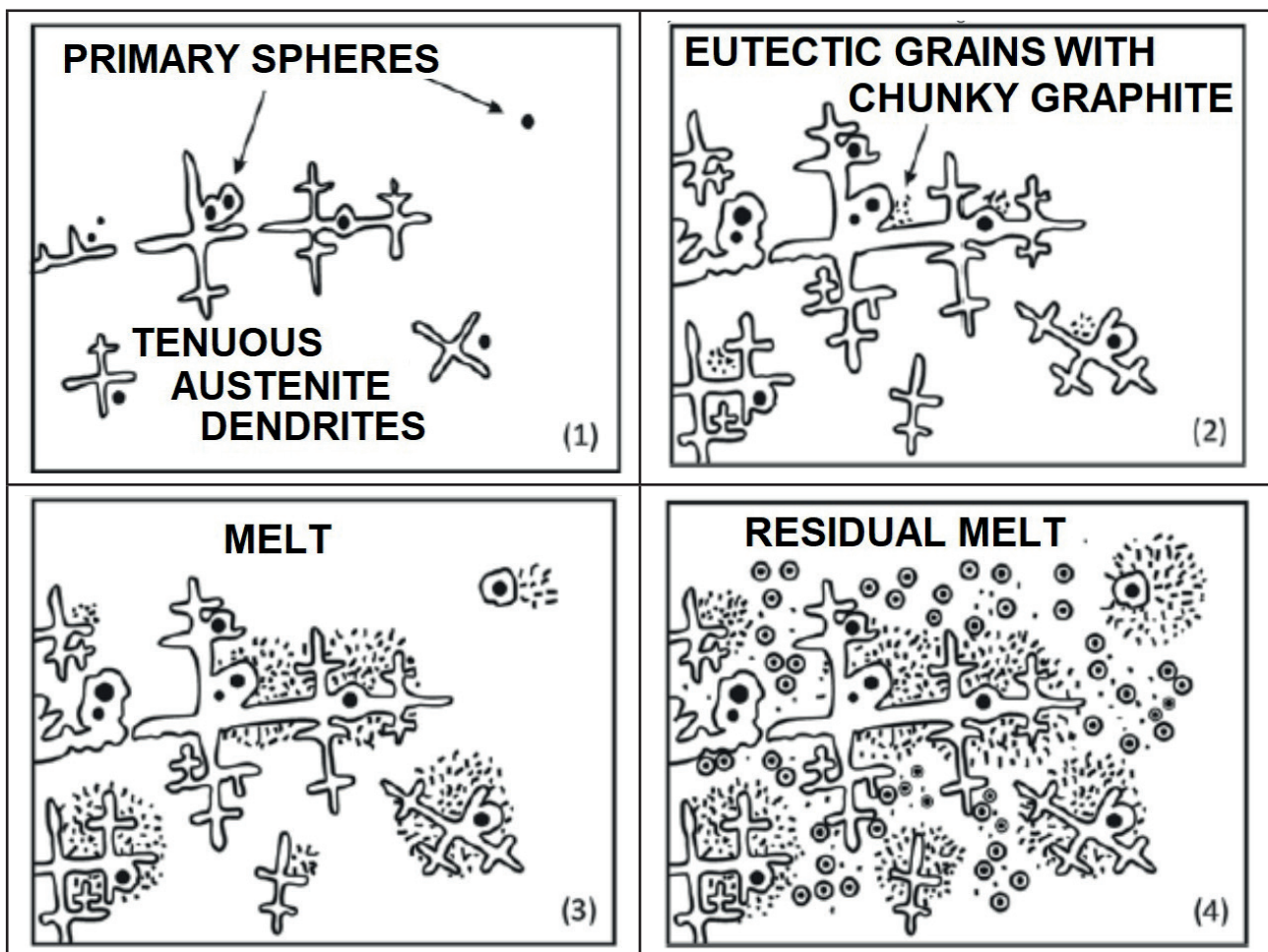
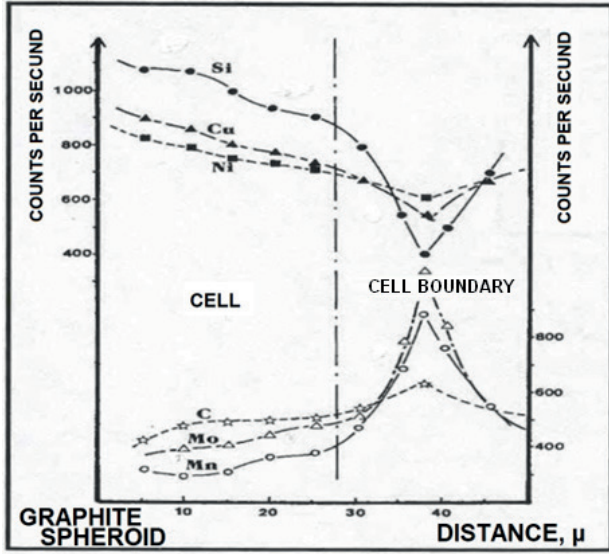


Fig. 1. Crystallization diagram of chunky graphite [1]. Explanation 1–4 in text

a)



b)

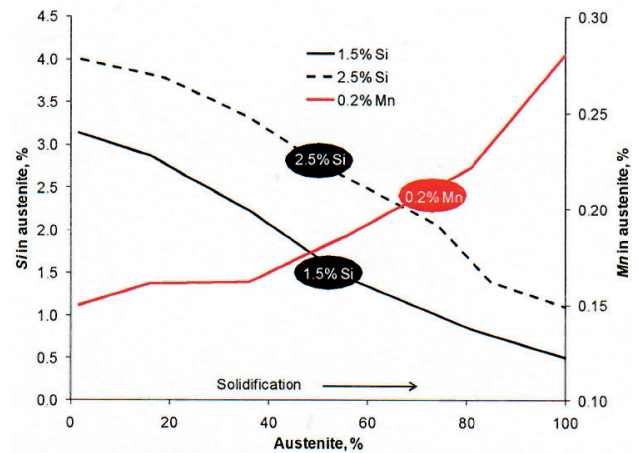


Fig. 2. Segregation of components in austenite in the area of spheroidal graphite: a) changes in concentration as a function of distance from the surface of the spheroidal graphite [2]; b) changes in the content of Si and Mn at the crystallization front depending on the degree of crystallization advancement [10]

Table 1

Segregation coefficient for the austenite structure in nodular cast iron [9]

Element	Si	Mn	Mg	Cu	Cr	Ni	Mo
K_s^*	2.27	0.29–0.59	0.387	5.10	0.108	1.82	0.0053

* K_s for nodular cast iron (sand mould $\varnothing = 30$ mm bar)

Therefore, silicon segregation should be considered:

- in crystallizing austenite dendrite [9],
- in the area of separated spheroid graphite [2, 10].

It seems that the negative segregation of silicon may strongly promote the formation of chunky graphite in cast iron containing levels of this element above 4%. By examining the microstructures, it could be clearly observed that the content of chunky graphite in the conical casting with dimensions of $D = 300$ mm and $H = 350$ mm with 3.5% Si does not increase from edge to centre, but on the contrary [11]. Reverse macro-segregation of silicon can be used to explain such micro-structural changes.

A number of studies have indicated that the formation of chunky graphite in ductile cast iron decreases with increasing cooling rates and low levels of rare earth (RE) additives, increases with increasing silicon content in the alloy, and is not sensitive to carbon equivalent [12].

Other research results indicate that there is no clear impact of some process parameters on the tendency to form chunky graphite in ductile cast iron. In high-silicon cast iron, after introducing a controlled amount of rare earth (RE) additives into standard materials, the occurrence of chunky graphite was unexpectedly reduced. Also the addition of small amounts of antimony to the liquid alloy, which is Mg treated with RE compounds, also stabilized the precipitation of graphite [13, 14]. These are put for-

ward on the interaction of strong nodularizer, such as Mg nodulizer with rare earth metals like antimony, which is a graphite denodularization, which is considered one of the trace elements unfavourable for ductile iron. Opinions are divided regarding the order in which spheroidal graphite and chunky graphite are released during the crystallization of cast iron.

Chunky graphite may occur as an intercellular and cellular form [15]. A common morphology of chunky graphite is a characteristic dendritic arrangement indicating the nature of the primary crystallization of cast iron.

The presented research is an introduction to the search for a stable technology for the production of silicon reinforced ductile iron castings. This utilitarian aspect is preceded by the cognitive aspect of the phenomena occurring in the liquid alloy in the furnace, during post-furnace processing and crystallization in the casting mould.

2. SCOPE OF RESEARCH

Pilot studies were carried out in foundry conditions regarding the influence of process parameters on the structure and mechanical properties of silicon-reinforced cast iron with spheroidal graphite. The research analysed:

- the effect of Mg nodulizers with and without RE,
- the effect of secondary inoculation with Bi and Ultraseed,
- the effect of addition microalloys Sb, V and Nb.

Cast iron was melted in an induction furnace with a capacity of 150 kg. The input consisted of pig iron (34%), steel scrap (30%) and ductile iron scrap (35%). Nodularization was carried out using the tundish cover method with magnesium (6% Mg). The primary inoculation was carried out with a barium inoculant in the amount of 0.4% while pouring the liquid alloy into the pouring ladle. Antimony and ferroalloys Fe-V (80% of V) and Fe-Nb (63% of Nb) were also introduced to the stream. Secondary inoculation was carried out in the stream by pouring cast iron into self-hardening sand moulds in the amount of 0.15%. The moulds of 4 test ingots with shapes according to EN 1563, Y12.5, Y25, Y50 and cylinder with diameter $d = 25$ mm were poured.

Mechanical properties were determined on the standard tensile samples with working part diameter 14 mm and length 70 mm using a ZwickRoell Z250 testing machine with a tensile diagram. The morphology of graphite was assessed using the MA100 NICON optical microscope, and an electron microscope TESCAN VEGA3 with the EDS system was used to assess the microstructure.

3. RESEARCH RESULTS

Chunky graphite occurs in cast iron in various forms. It is distributed in the inter-dendritic space and in clusters between the precipitates of spheroidal graphite (Fig. 3).

In cast iron containing more than 4% Si, degenerate graphite was observed in ingots with a thickness of 50 mm. A treatment Mg without RE, without the addition of antimony, with Bi inoculant as a secondary was used (Fig. 4a). Cast iron from smelting using magnesium alloy with RE (Ce, La), inoculation with Ultraseed (Ce) and antimony crystallized in a 50 mm thick ingot with spheroidal graphite (Fig. 4b). With a similar Mg content and ferritic structure, $R_m > 600$ MPa and A elongation of 15% were obtained for cast iron with RE and Sb. Various forms of graphite are summarized in Figure 5.

Chunky graphite appeared in islands next to spheroidal graphite in the external cross-sections of strength samples in the areas of their decohesion. Spheroidal graphite was observed in the axis of the samples (Fig. 6). These areas observed under an electron microscope revealed an increased concentration of silicon in the chunky graphite area (Fig. 6 and Fig. 7).

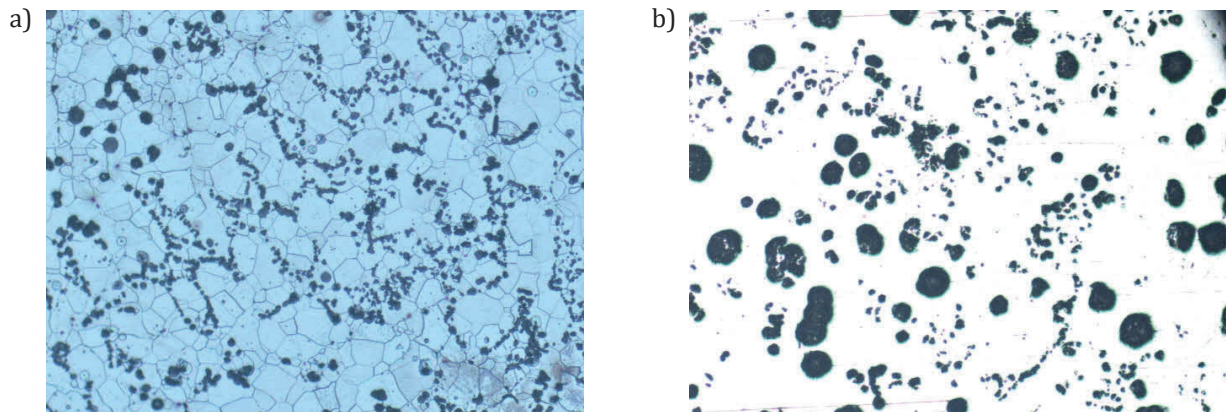
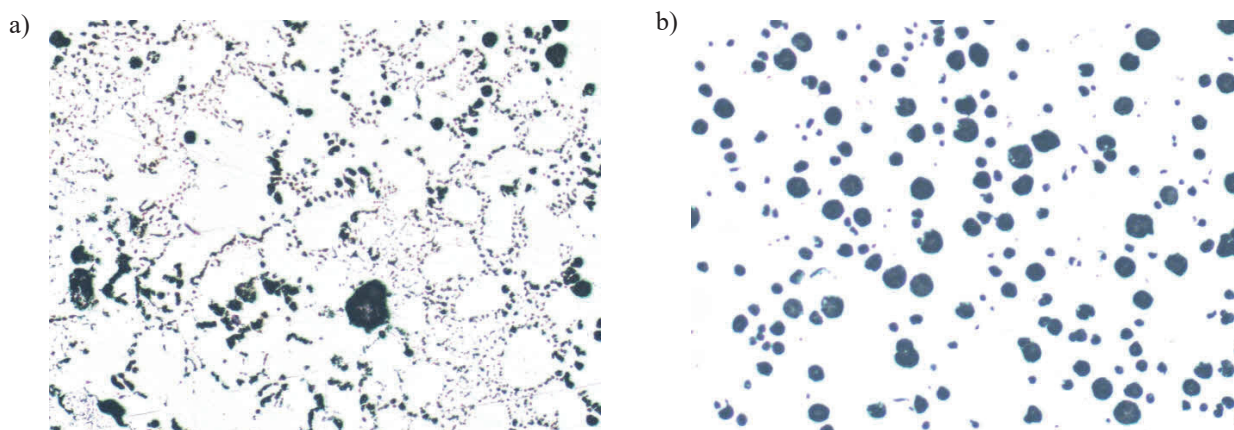


Fig. 3. Chunky graphite: a) dendritic composition (Nital etching); b) coexisting forms of chunky and spheroidal graphite



Number of precipitates [1/mm²] 653
Degree of spheroidization [%] 77.5
Area fraction of graphite [%] 10.6
Ferrite fraction in the matrix [%] 100
 C = 2.99%; Si = 4.31%; Sb = 0.0013;
 Ce = 0.001%; La = 0.0001%
 $R_m = 501$ MPa; A = 0.8%
 FeSiMg /Inoculant with Bi; Sb = 0,0008%

Number of precipitates [1/mm²] 327
Degree of spheroidization [%] 94.7
Area fraction of graphite [%] 14.5
Ferrite fraction in the matrix [%] 100
 C = 2.77%; Si = 4.33%; Sb = 0.0083%;
 Ce = 0.010%; La = 0.0051%
 $R_m = 629$ MPa; A = 15.0%
 FeSiMg(RE)/Inoculant Ultraseed and Sb = 0,0241%

Fig. 4. Morphology of graphite in strength samples taken from the Y50 mm ingot: a) chunky graphite; b) spheroidal graphite

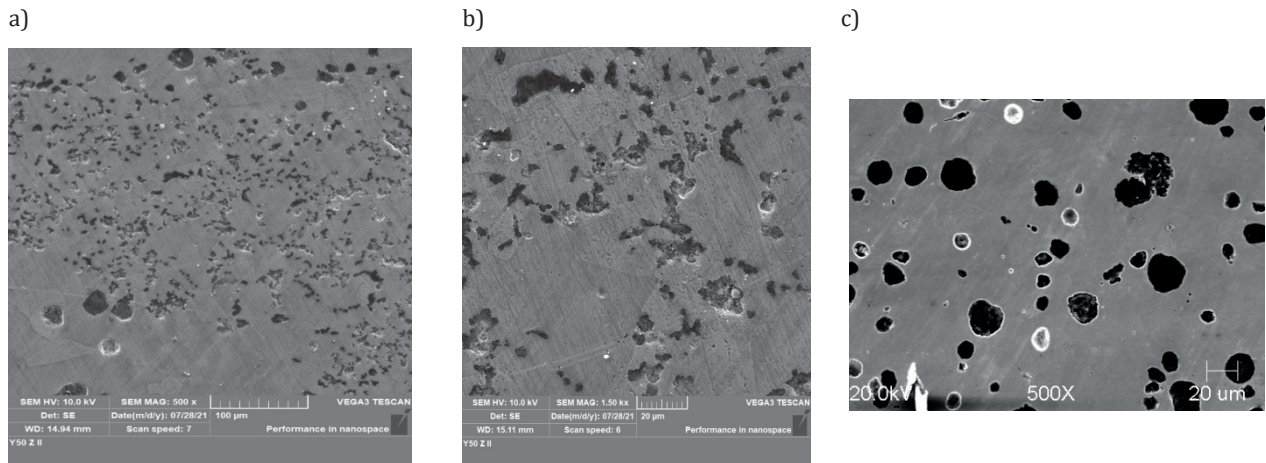


Fig. 5. Chunky graphite and spheroidal graphite forms: (a, b) C = 2.99%; Si = 4.31%; Sb = 0.0013%; c) C = 2.77%; Si = 4.33%; Sb = 0.0083%

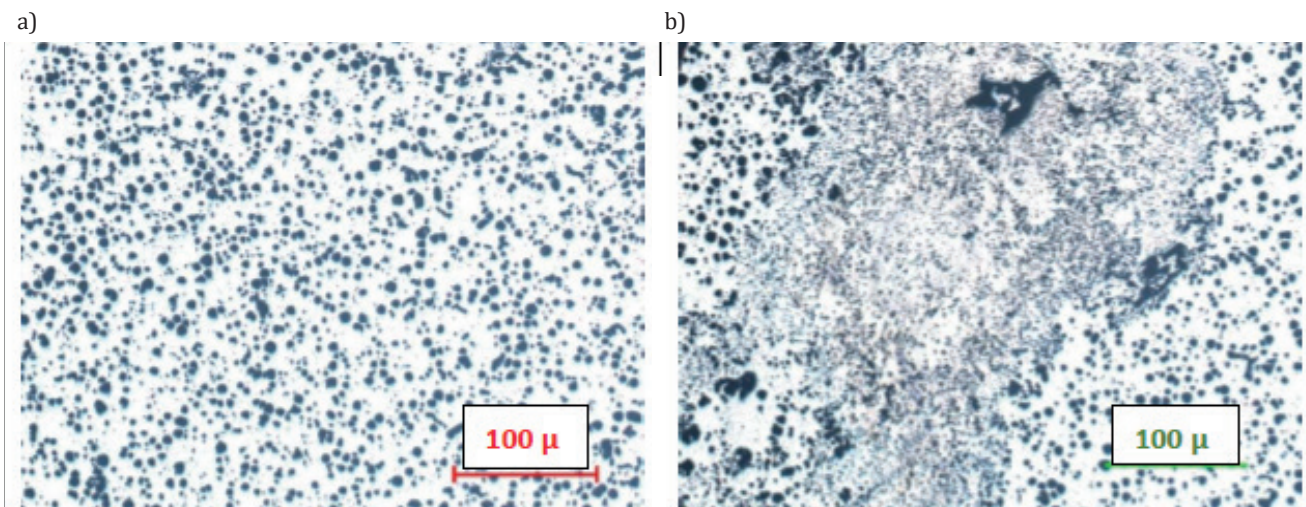


Fig. 6. Chunky graphite, optical microscope. Shaft casting $d = 25$ mm, a) centre of the specimen; b) edge of the specimen

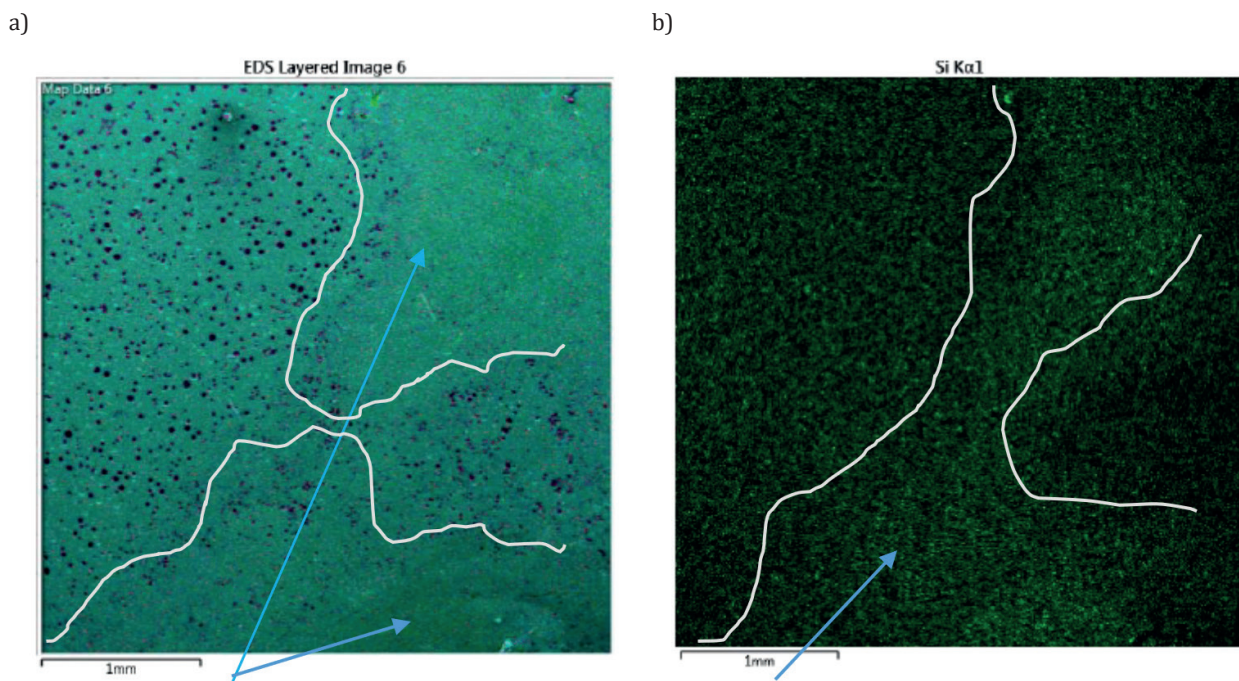


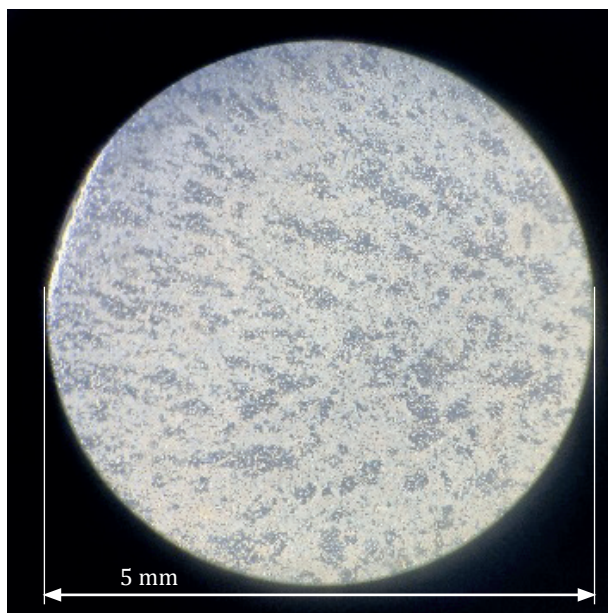
Fig. 7. Graphite morphology, electron microscope (EDS): a) chunky graphite, b) Si distribution in the chunky graphite area

Cast iron of the GJS 600-10 grade, spheroidized with magnesium alloys with rare earth metals and modified with antimony, obtains high values of elongation A, almost twice as high as those indicated in the standard, both in thin walls (up to 12 mm) and in a 50 mm thick ingot. A small technological reserve of the R_m value was obtained in relation to requirements according to EN 1563 (up to 630 MPa). The developed technology should guarantee strengths exceeding 650 MPa, so the strengthening of cast iron with silicon was insufficient.

One of the methods for strengthening metal alloys is grain refinement of the matrix. Methods known in the ma-

terials engineering of steel and cast steel include the introduction of micro-additives to the alloy. Therefore, the liquid alloy was modified with additions of vanadium and niobium. This treatment turned out to be effective. A more favourable macrostructure of cast iron with V and Nb was obtained (Fig. 8), a greater number of fine graphite precipitations was obtained (Fig. 9), and, above all, an increase in the value of the R_m parameter was achieved (670–690 MPa). Unfortunately, the solid solution strengthening of the matrix had a negative impact on the elongation values, which decreased to the minimum level required for a 50 mm thick wall – approx. 8%.

a)

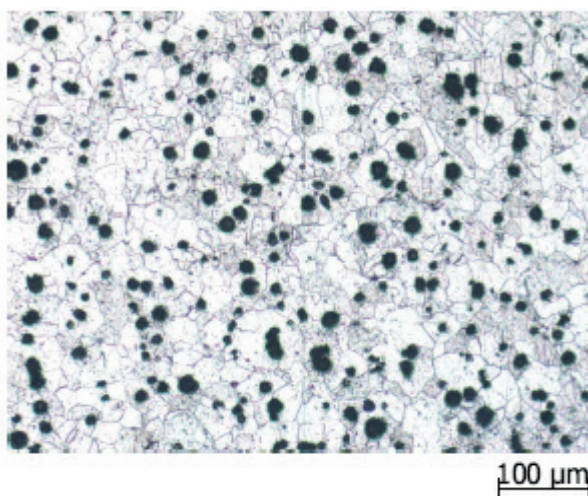


b)



Fig. 8. Effect of modification with vanadium and niobium on the macrostructure of cast iron (etching with Oberhoffer's reagent): a) cast iron without micro-additives; b) cast iron modified with V = 0,110% and Nb = 0,043% (see Fig. 9b)

a)



b)

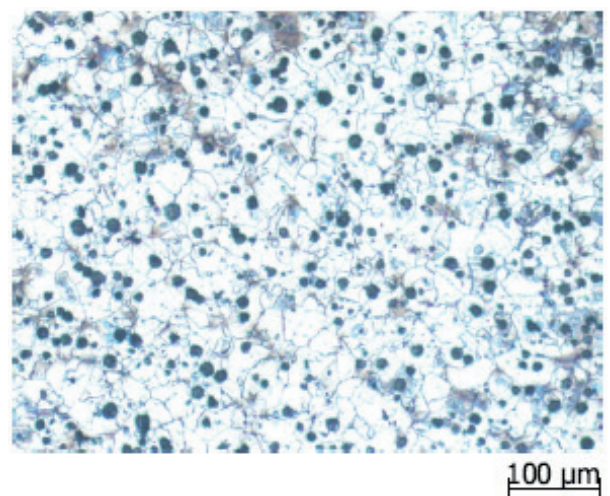


Fig. 9. The influence of V and Nb additives on the structure and strength properties of ductile iron solution strengthened by silicon: a) Y25; 409 1/mm²; R_m = 611MPa; A = 18.3%; Sb = 0.029%; V = 0.008%; Nb = 0.003%; b) Y25; 510 1/mm²; R_m = 690MPa; A = 12.7%; Sb = 0.024%; V = 0.110%; Nb = 0.043%

4. ANALYSIS

Pilot tests of ductile iron containing above 4% silicon indicate that the minimum values of strength and elongation required by the standard can be obtained, provided that chunky graphite is eliminated from the structure of cast iron. This graphite was present in the thickest walls of the test ingots (50 mm), as well as in the sprue zones. Magnesium carriers used in the post-furnace treatment containing small amounts of elements such as Ce and La, together with the micro-addition of antimony, eliminated chunky graphite from the structure of the cast iron. Ultra-seed (containing Ce, S and O) was found to be the more beneficial of the two recommended inoculants used for secondary inoculation compared to bismuth (Fig. 4). To limit the impact of RE and Ce on the final microstructure Sb is usually added. Here Sb acts like a diffusion barrier around the graphite and leads to higher nodularity and nodule counts [16].

The effect of high silicon content on the generation of chunky graphite, known from the literature, was revealed in the area of degenerated graphite (compare Fig. 6 and Fig. 7). Its tendency to negative segregation in the casting may be one of the reasons for the occurrence of this form of graphite, which reduces the mechanical properties of cast iron (Figs. 2 and 7).

The introduction of small amounts of V and Nb into the liquid alloy may result, as in the case of steel, in the refinement of the austenite grain in iron castings, which in secondary crystallization affects the refinement of the ferrite grain (Fig. 9). A smaller ferrite grain strengthens the alloy (Hall-Petch relationship; $\sigma_y = \sigma_0 + kd^{-1/2}$) [17, 18]. The introduction of modifier pads with a crystal lattice consistent with the austenite lattice may increase the number of crystallization nuclei. In the analysed cast iron, this resulted in the fragmentation of austenite dendrites (Fig. 1), reducing the negative effect of silicon segregation. This phenomenon is confirmed by the change in the microstructure of modified cast iron from clearly dendritic to non-axial (Fig. 8).

5. SUMMARY

The pilot tests conducted indicated the further direction of research on silicon-reinforced cast iron. The introduced graphite modifiers, the use of a despheroidizer, namely antimony, and the use of primary structure modifiers (V and Nb) are methods of eliminating graphite degeneration.

The process stability of silicon-reinforced ductile cast iron can be ensured by introducing a combination of graphitizing modification and austenite modification into the technological process. Such technological procedures introduce pads into the liquid alloy to nucleate both components of the microstructure of the cast iron composite, namely: graphite and austenite.

The research was carried out as part of the co-financing of the „Fast Path” project (NCBR), no. POIR.01.01.01-00-1303/19.

REFERENCES

- [1] Baer W. (2020). Chunky graphite in ferritic spheroidal graphite cast iron: formation, prevention, characterization, impact on properties: An overview. *International Journal of Metal Casting*, 14(2), 454–488. DOI: <https://doi.org/10.1007/s40962-019-00363-8>.
- [2] Muratore E.C. (2006). *Manganese Another Look at Segregation*. Sorelmetal T. S. 107, Rio Tinto Iron & Titanium Inc.
- [3] Udroui A. (2013). Die Keil-Theorie. Ein neuer Ansatz zur Erklärung der Bildung von Chunky-Graphit in Gusseisen mit Kugelgraphit. *Giesserei Rundschau*, 60, 356–374.
- [4] Liu P.C., Li C.L., Wu D.H. & Loper C.R. (1983). SEM study of chunky graphite in heavy section ductile iron. *AFS Transactions*, 91, 119–126.
- [5] Zhou J., Schmitz W. & Engler S. (1987). Untersuchung der Gefügebildung von Gußeisen mit Kugelgraphit bei langsamer Erstarrung. *Giessereiforschung*, 39, 55–70.
- [6] Gagné M. & Argo D. (1989). Heavy section ductile cast iron castings part I and part II. In: *Proceedings of an International Conference on Advanced Casting Technology, Kalamazoo, Michigan, USA, November 12–14*, ASM International, USA, 231–256.
- [7] Itofuji H. & Uchikawa H. (1990). Formation mechanism of chunky graphite in heavy-section ductile cast iron, *AFS Transactions*, 98(90–42), 429–448.
- [8] Källbom R., Hamberg K., Wessén M. & Björkegren L.-E. (2005). On the solidification sequence of ductile iron castings containing chunky graphite. *Materials Science and Engineering A*, 413, 346–351. DOI: <https://doi.org/10.1016/j.msea.2005.08.210>.
- [9] Azevedo dos Anjos V.E. (2015). *Use of Thermal Analysis to Control the Solidification Morphology of Nodular Cast Irons and Reduce Feeding Needs*. Universität Duisburg-Essen, Abteilung Maschinenbau und Verfahrenstechnik. Retrieved from: https://duepublico2.uni-due.de/servlets/MCRFileNodeServlet/duepublico_derivate_00039710/Anjos_Vitor_Diss.pdf [25.11.2024].
- [10] Lekakh S.N., Richards V.L. & Medvedeva N. (2012). Effect of Si segregation on low temperature toughness of ductile iron. *Transactions of AFS*, 120, 319–327.
- [11] Mihalic Pokopec I., Mrvar P. & Bauer B. (2018). Influence of chunky graphite on latent heat. *Materiali in tehnologije / Materials and technology*, 52(1), 59–65. DOI: <https://doi.org/10.17222/mit.2017.122>.
- [12] Torre U., de la, Lacaze J. & Sertucha J. (2016). Chunky graphite formation in ductile cast irons: effect of silicon, carbon and rare earths. *International Journal of Materials Research*, 107(11), 1041–1050. DOI: <https://doi.org/10.3139/146.111434>.
- [13] Sertucha J., Artola G., de La Torre U. & Lacaze J. (2020). Chunky graphite in low and high silicon spheroidal graphite cast irons – occurrence, control and effect on mechanical properties. *Materials*. 13(23), 5402. DOI: <https://doi.org/10.3390/ma13235402>.
- [14] Larrañaga P., Asenjo I., Sertucha J., Suarez R., Ferrer I. & Lacaze J. (2009). Effect of Antimony and Cerium on the formation of chunky graphite during solidification of heavy-section castings of near-eutectic spheroidal graphite irons. *Metallurgical and Materials Transactions A*, 40(3), 654–661. DOI: <https://doi.org/10.1007/s11661-008-9731-y>.

- [15] Knustad O., Magnusson Åberg L. & Plowman A. (2015). Chunky graphite: Formation and prevention in heavy-section castings. *AFS Transactions. 119th American Foundry Society MetalCasting Congress, Columbus, Ohio*.
- [16] Borgström H. & Furlakidis V. (2014). A review of side-lined chunky graphite phenomena. *10th International Symposium on the Science and Processing of Cast Iron – SPCI10*. Mar Del Plata Argentina: INTEMA, pp. 36–42.
- [17] Baker T.N. (2016). Microalloyed steels. *Ironmaking & Steelmaking*, 43(4), 264–307. DOI: <https://doi.org/10.1179/1743281215Y0000000063>.
- [18] Opiela M. (2021). Thermodynamic analysis of precipitation process of MX-type, phases in high strength low alloy steels. *Advances in Science and Technology – Research Journal*, 15(2), 90–100. DOI: <https://doi.org/10.12913/22998624/135514>.